Self-consistent description of Andreev bound states in Josephson quantum dot devices

Tobias Meng and Serge Florens

Institut Néel, CNRS and Université Joseph Fourier, 25 Avenue des Martyrs, 38042 Grenoble, France

Pascal Simon

Laboratoire de Physique et Modélisation des Milieux Condensés, CNRS and Université Joseph Fourier,
BP 166, 38042 Grenoble, France;

Department of Physics, University of Basel, Klingelbergstrasse 82, 4056 Basel, Switzerland;

and Laboratoire de Physique des Solides, CNRS UMR-8502, Université Paris Sud, 91405 Orsay Cedex, France

We develop a general perturbative framework based on a *superconducting atomic limit* for the description of Andreev bound states (ABS) in interacting quantum dots connected to superconducting leads. A local effective Hamiltonian for dressed ABS, including both the atomic (or molecular) levels and the induced proximity effect on the dot is argued to be a natural starting point. A self-consistent expansion in single-particle tunneling events is shown to provide accurate results even in regimes where the superconducting gap is smaller than the atomic energies, as demonstrated by a comparison to recent numerical renormalization group calculations. This simple formulation may have bearings for interpreting Andreev spectroscopic experiments in superconducting devices, such as scanning tunnel microscope measurements on carbon nanotubes or radiative emission in optical quantum dots.

I. INTRODUCTION

When a quantum dot is connected to superconducting electrodes, the proximity effect drastically modifies the dot's electronic structure due to the local formation of Cooper pairs. The density of states on the dot thus exhibits a gap so that the formation of discrete subgap states arises.[1] These Andreev bound states (ABS) play certainly an important role as they may contribute a large part of the spectral weight[2] and carry most of the Josephson current.[3] A physical understanding of the ABS requires to characterize how these states are connected to the atomic (or molecular) levels of the uncoupled quantum dot and to describe quantitatively their evolution as a function of several parameters such as gate voltage, Coulomb interaction, tunnel couplings, and superconducting gap. Whereas the ABS have been observed in metal-superconductor hybrid structures,[4] no direct spectroscopy has so far been achieved in quantum dot systems. Andreev bound states come in pairs, one state above and one below the Fermi level, forming a two-level system. Consequently, recent interest in the spectroscopy of the bound states has also been stimulated by proposals to use the latter as a qubit.[5] At present, several routes have been suggested such as scanning tunnel microscope (STM) measurements on carbon nanotubes,[6] microwave cavity coupling,[7] visible-light emission using a Josephon diode,[8] or noise experiments.[9]

Experimentally, superconducting quantum dots can be realized with carbon nanotubes junctions or semiconducting InAs islands. It has been shown that quantum dots connected to superconducting electrodes can be tuned from a Coulomb blockade regime, to a Kondo regime,[10,11] and to a weakly-interacting Fabry-Perot regime by changing local gate voltages.[12] The Josephson current at zero bias and multiple Andreev reflections at finite bias voltage have been measured in such devices.[12–15] The transition from a zero junction to a π junction, namely, a reversal in the sign of the Josephson current[16] has also been observed when a magnetic moment forms on the dot.[17–20] As a possible application of superconducting junctions, nano superconducting quantum interference devices have also been fabricated.[19]

An exact theoretical description of a quantum dot coupled to superconducting leads is only possible when the Coulomb interaction is fully neglected. Hence the interacting single-dot system, as described by the Anderson model with superconducting electrodes, has been so far analyzed by treating the Coulomb interaction with various analytical schemes such as the mean-field theory,[21–23] the perturbation expansion in the Coulomb interaction,[24] or in the tunnel coupling.[16] Nonperturbative calculations, using the noncrossing approximation (NCA),[25,26] or the functional renormalization group,[27] as well as numerical simulations based on the numerical renormalization group (NRG),[2,27–31] or quantum Monte Carlo[32,33] have also been developed.

None of the analytical approaches mentioned above is able to describe entirely the physics of a quantum dot coupled to superconducting leads. Whereas lowest-order perturbation expansions in the tunnel coupling will hardly capture the proximity effect induced by the electrodes[34] and need to be pushed to higher orders,[35] mean-field and weak-interaction approaches will miss the Kondo effect. NRG calculations on the other hand can capture the physics of such a system over a wide range of parameters but are numerically demanding and not easily portable to more complex molecular systems. More importantly, in the view of describing the ABS alone, none of these techniques does provide a simple physical picture. Henceforth we will develop in this paper a perturbative approach based on an effective local Hamiltonian for dressed ABS, that extends the limit of large superconducting gap proposed previously,[36,37] which was used by many authors.[2,6,8,24,38–41] This approach will illuminate the nature of the ABS in interacting quantum dots, which can be generally viewed as renormalized superconducting atomic

states. This will provide as well a simple analytical framework that is accurate in the most relevant cases and that may thus be useful for interpreting future spectroscopic experiments. In particular, calculations provided in the proposals of Refs. 6 and 8 only *qualitatively* apply in realistic situations where the gap is comparable or smaller that the atomic energies even when the gap is large compared to the hybridization to the electrodes. This interesting regime is precisely the one that we want to address in the present work. In addition, we note that our formalism, which incorporates the atomic (or molecular) levels from the outset, can easily be extended to describe more complex systems, as for instance superconducting double quantum dots or molecules with more complicated orbital structure (see, e.g., Refs. 42–45).

We organize our paper as follows. In Sec. II, the system is mapped onto an effective local Hamiltonian, similarly to the widely used atomic limit but including the proximity effects due to the superconducting leads. In Sec. III, the perturbation theory around this limit is set up and self-consistent equations for the ABS energy renormalizations are derived in order to extend the validity of the bare perturbative approach. Sec. IV illustrates how this expansion can describe ABS in superconducting quantum dots over a wide range of parameters by a comparison to available NRG data.[2,30]

II. THEORETICAL FORMULATION

A. Model

We focus in this paper on a single-level quantum dot coupled to superconducting leads, which is relevant experimentally for molecular junctions with large single-electron level spacing. A simple Hamiltonian able to describe such a system is given by the superconducting Anderson model

$$H = \sum_{i=L,R} H_i + H_d + \sum_{i=L,R} H_{T_i}, \qquad (1)$$

where

$$H_i = \sum_{\vec{k},\sigma} \epsilon_{\vec{k}} c_{\vec{k},\sigma,i}^\dagger c_{\vec{k},\sigma,i} - \sum_{\vec{k}} (\Delta_i c_{\vec{k},\uparrow,i}^\dagger c_{-\vec{k},\downarrow,i}^\dagger + \text{H.c.}),$$

$$H_d = \sum_\sigma \epsilon_d d_\sigma^\dagger d_\sigma + U n_\uparrow n_\downarrow,$$

$$H_{T_i} = \sum_{\vec{k},\sigma} (t d_\sigma^\dagger c_{\vec{k},\sigma,i} + \text{H.c.}).$$

In the above equations, d_σ is the annihilation operator of an electron with spin σ on the dot, $c_{\vec{k},\sigma,i}$ that of an electron with spin σ and wave vector $\vec{k}$ in the lead $i=L,R$ and $n_\sigma=d_\sigma^\dagger d_\sigma$. The leads are assumed to be described by standard s-wave BCS Hamiltonians H_i with superconducting gaps $\Delta_i=\Delta e^{i\varphi_i}$. The phase difference of the latter is noted $\varphi=\varphi_L-\varphi_R$. Furthermore, the leads are assumed to have flat and symmetric conduction bands, i.e., the kinetic energy $\epsilon_{\vec{k},i}$ measured from the Fermi-level ranges in $[-D,D]$ and the density of states is $\rho_0=1/(2D)$. We assume $\vec{k}$-independent and symmetric-tunneling amplitudes t between the dot and both superconducting leads. The dot has a level energy ϵ_d and Coulomb interaction U. Experimentally, the crucial characteristic energy scales, namely, Coulomb interaction U, total hybridization $\Gamma=2\pi t^2\rho_0$ and gap Δ, are typically all of the same order of magnitude,[19,46] providing a challenge for analytical methods.

The physics of the quantum dot can be described via its Green's function,

$$\hat{G}_{d,d}(\tau) = -\langle T_\tau \Psi_d(\tau)\Psi_d^\dagger(0)\rangle, \qquad (2)$$

where the Nambu spinor

$$\Psi_d(\tau) = \begin{bmatrix} d_\uparrow(\tau) \\ d_\downarrow^\dagger(\tau) \end{bmatrix}$$

has been introduced. Because we will only be interested in stationary equilibrium physics, $\hat{G}_{d,d}(\tau)$ shall be computed in the Matsubara frequency formalism.

B. Effective local Hamiltonian

As the above Hamiltonian has no exact solution, some approximations must be made. Among the physical ingredients we want to include in a nonperturbative way is the local pairing on the dot that is crucial for the evolution of the Andreev bound states. Furthermore, the Coulomb interaction shall be taken into account in an exact manner in order to describe the atomic states faithfully and to highlight how these are adiabatically connected to the ABS. However, the usual development in weak tunnel coupling t around the atomic limit[16] is not sufficient to describe the proximity effect at lowest order. Therefore, we shall consider in what follows an expansion around a *superconducting atomic limit*.

Such simple solvable limiting case of the model in Eq. (1) is often referred to as the limit of large gap $\Delta \to \infty$ and has been discussed previously.[2,24,36,38] Expansions for finite Δ have not however been discussed to our knowledge and are the topic of this paper. We emphasize from the outset [see Eq. (4) below], that the superconducting atomic limit as used normally in the literature corresponds to the limit $D \to \infty$ (i.e., infinite electronic bandwidth), taken before $\Delta \to \infty$. The order of the two limits is crucial: if the limit $\Delta \to \infty$ was to be taken first, the dot would be completely decoupled from the leads and the proximity effect would be lost so that the limit of infinite gap would reduce to the usual atomic limit. As will be shown now, the superconducting atomic limit should rather be interpreted as a low-frequency expansion, i.e., a limit where the gap is much larger than the characteristic frequencies of the dot.

We start off by deriving the Green's function defined in Eq. (2) using the equations of motion. Thereby, the Coulomb interaction U will at first be omitted for the sake of clarity. Note that in the end, U will simply give an extra contribution which adds to the effective Hamiltonian. Fourier transformation straightforwardly yields

$$\hat{G}_{d,d}^{-1}(i\omega_n) = i\omega_n \mathbb{1} - \epsilon_d \hat{\sigma}_z - t^2 \sum_{\vec{k},i} \hat{\sigma}_x \hat{G}_{\vec{k}i,\vec{k}i}^0(i\omega_n)\hat{\sigma}_x. \qquad (3)$$

In Eq. (3), ω_n is a fermionic Matsubara frequency, $\hat{G}_{\vec{k}i,\vec{k}i}^0(i\omega_n)$ is the bare Green's function in Nambu space of electrons

with a wave vector $\vec{k}$ in the lead i, and the Pauli matrices $\hat{\sigma}_\alpha$ have been introduced. Transforming the sum over wave vectors $\vec{k}$ into an integral over energies yields the $\vec{k}$-summed "quasiclassical" Green's function,

$$\sum_{\vec{k}} \hat{G}^0_{\vec{k}i,\vec{k}i}(i\omega_n) = 2\rho_0 \arctan\left(\frac{D}{\sqrt{\omega_n^2 + \Delta^2}}\right)$$
$$\times \frac{1}{\sqrt{\omega_n^2 + \Delta^2}} \begin{pmatrix} -i\omega_n & \Delta e^{i\varphi_i} \\ \Delta e^{-i\varphi_i} & -i\omega_n \end{pmatrix}. \quad (4)$$

In the limit $\omega_n \ll \Delta$, the Green's function in Eq. (4) becomes purely *static* and reduces to

$$\sum_{\vec{k}} \hat{G}^0_{\vec{k}i,\vec{k}i}(i\omega_n) = 2\rho_0 \arctan\left(\frac{D}{\Delta}\right) \begin{pmatrix} 0 & e^{i\varphi_i} \\ e^{-i\varphi_i} & 0 \end{pmatrix}. \quad (5)$$

Note that the low-frequency limit we consider here yields a Green's function that indeed depends on the finite bandwidth D and this shows that the limit $\Delta \to \infty$ shall not be taken for the proximity effect to survive. In what follows, we will therefore keep both D and Δ finite. Plugging Eq. (5) into the Green's function $\hat{G}_{d,d}(i\omega_n)$ leads to the same result as would have been obtained with the effective local Hamiltonian

$$H^0_{\text{eff}} = \sum_\sigma \epsilon_d d^\dagger_\sigma d_\sigma - (\Gamma_\varphi e^{i(\varphi_L + \varphi_R/2)} d^\dagger_\uparrow d^\dagger_\downarrow + \text{H.c.}), \quad (6)$$

where the local-pairing amplitude induced by the leads on the dot reads as

$$\Gamma_\varphi = \Gamma \frac{2}{\pi} \arctan\left(\frac{D}{\Delta}\right) \cos\left(\frac{\varphi}{2}\right). \quad (7)$$

which explicitly depends on the ratio D/Δ. By an appropriate gauge transformation for the operators d_σ, it is always possible to choose $\Gamma_\varphi e^{i(\varphi_L+\varphi_R/2)} = |\Gamma_\varphi|$, as shall be done from now on. The complete local effective Hamiltonian is obtained when the Coulomb interaction is taken into account again. Defining $\xi_d = \epsilon_d + \frac{U}{2}$, the energy level of the dot is shifted such that the Hamiltonian clearly exhibits particle-hole symmetry for $\xi_d = 0$,

$$H_{\text{eff}} = \sum_\sigma \xi_d d^\dagger_\sigma d_\sigma - |\Gamma_\varphi|(d^\dagger_\uparrow d^\dagger_\downarrow + \text{H.c.}) + \frac{U}{2}\left(\sum_\sigma d^\dagger_\sigma d_\sigma - 1\right)^2. \quad (8)$$

The physical interpretation of this effective local Hamiltonian is simple. For finite gap, the quantum dot is coupled to both the Cooper pairs and the quasiparticles in the leads. The Cooper pairs, which lie at the Fermi level, are responsible for the proximity effect. The quasiparticles give rise to conduction electrons excitations with energies higher than the gap Δ. In the limit $\omega_n \ll \Delta$, the quasiparticles are far in energy and the coupling between them and the dot vanishes, which greatly simplifies the physics and makes an exact solution possible. Yet, as the dot is still coupled to the Cooper pairs at the Fermi level, the proximity effect survives with a local pairing term proportional to the hybridization Γ between dot and leads.
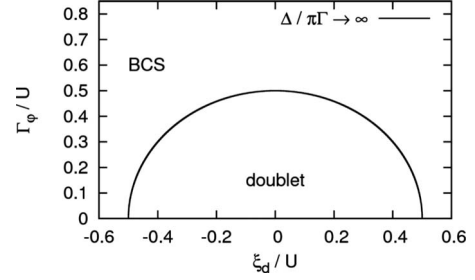

FIG. 1. Phase diagram of a simple dot with Coulomb interaction U, energy level ξ_d and hybridization Γ to superconducting electrodes in the effective local limit. The transition line corresponds to $E^0_\sigma = E^0_-$.

C. Spectrum of the effective local Hamiltonian

As the Coulomb interaction simply yields an extra energy shift of $U/2$ for both empty and doubly occupied dot, the eigenvectors and eigenvalues of the local effective Hamiltonian in Eq. (8) are readily obtained by a Bogoliubov transformation,[2] in perfect analogy with solution of the BCS Hamiltonian. H_{eff} has thus four eigenstates, the singly occupied spin 1/2 states $|\uparrow\rangle$ and $|\downarrow\rangle$ with energy $E^0_\uparrow = E^0_\downarrow = \xi_d$, and two BCS-like states given by

$$|+\rangle = u|\uparrow\downarrow\rangle + v^*|0\rangle,$$
$$|-\rangle = -v^*|\uparrow\downarrow\rangle + u|0\rangle, \quad (9)$$

where $|0\rangle$ denotes the empty dot and $|\uparrow\downarrow\rangle$ the doubly occupied dot. The amplitudes u and v can always be chosen to be real with $u = 1/2\sqrt{1 + \xi_d/\sqrt{\xi_d^2 + \Gamma_\varphi^2}}$ and $v = 1/2\sqrt{1 - \xi_d/\sqrt{\xi_d^2 + \Gamma_\varphi^2}}$. The energies corresponding to these BCS-type states are $E^0_\pm = U/2 \pm \sqrt{\xi_d^2 + \Gamma_\varphi^2} + \xi_d$.

As E^0_+ is always larger than E^0_-, the effective local Hamiltonian has two possible ground states: the low-energy BCS-type state $|-\rangle$ or the degenerate spin 1/2 doublet $\{|\uparrow\rangle, |\downarrow\rangle\}$. In the $|-\rangle$ state, the energy is minimized for $\varphi = 0$. Thus, the spin-singlet phase corresponds to a zero junction (a result well known from the weak-coupling limit[16]). The transition between the singlet phase and the spin 1/2 doublet takes place at $\xi_d^2 + \Gamma_\varphi^2 = U^2/4$ and Fig. 1 shows the corresponding phase diagram for variable ξ_d, Γ_φ, and U. The state adopted by the quantum dot in the large-gap limit therefore results from a competition between the local pairing (induced by the proximity effect and characterized by the hybridization Γ) and the Coulomb interaction.

D. Andreev bound states

As outlined in Sec. I, the coupling to superconducting leads induces a gap in the spectral function of the dot inside which discrete Andreev bound states can form. The spectral function of the dot shows therefore sharp peaks, which could be measured by STM (Ref. 6) or microwave-optical[7,8] experiments as proposed recently. These peaks indicate addition energies at which an electron may enter (or leave) the dot and correspond therefore to transitions between states with n and $n \pm 1$ electrons. Hence, the ABS peaks in the

spectral function may be interpreted as transitions between the superconducting atomic levels of the dot $\{|\sigma\rangle, |+\rangle, |-\rangle\}$, possibly renormalized by single-particle tunneling events neglected in H_{eff} (to be included in the next section). Furthermore, transitions from a spin 1/2 doublet to a spin singlet necessarily involve an electron exchange between the dot and the superconducting leads. As the states $|-\rangle$ and $|+\rangle$ correspond to the superposition of an empty and doubly occupied dot, this electron exchange and the final singlet states can be understood within the Andreev reflection picture.

Putting everything together, our effective local Hamiltonian in Eq. (8) describes the energies of the Andreev bound states as transition energies from the spin 1/2 doublet to the spin-singlet states.[2,38] There are thus four Andreev bound states in the large-gap limit for the model Eq. (1), with energy $\pm a_0$ and $\pm b_0$ which read as

$$a_0 = E_-^0 - E_\sigma^0 = \frac{U}{2} - \sqrt{\xi_d^2 + \Gamma_\varphi^2}, \qquad (10)$$

$$b_0 = E_+^0 - E_\sigma^0 = \frac{U}{2} + \sqrt{\xi_d^2 + \Gamma_\varphi^2}. \qquad (11)$$

The $0/\pi$ transition corresponds to the crossing of the $|-\rangle$ and $|\sigma\rangle$ states, which occurs for $a_0 = 0$.

III. PERTURBATION EXPANSION AROUND THE EFFECTIVE LOCAL HAMILTONIAN

A. Perturbation theory

The effective Hamiltonian is not sufficient to obtain satisfying results for all regimes of parameters. First, H_{eff} only describes the $0/\pi$-junction transition due to the competition between a local-moment state (stabilized by the Coulomb blockade) and a spin singlet (induced by the proximity effect). However, if the Coulomb interaction is strong (i.e., $U \gg \Gamma, |\xi_d|$, and below the Kondo temperature), the local moment can be screened by the Kondo effect, which will compete with the superconducting gap for the 0-π transition so that a typical scaling in the ratio of the Kondo temperature to the gap Δ will appear. Also, the Josephson current in the π phase identically vanishes from H_{eff}, as the spin doublet does not disperse with the superconducting phase difference, a limitation of the large-gap limit. On a more quantitative basis, the experimental gap Δ is usually on the order of a few kelvins, which is also the typical scale for both Γ and U in carbon nanotube quantum dot devices.

In order to extend the description of the quantum dot's physics, energy corrections shall be calculated with a perturbation theory around the effective Hamiltonian in Eq. (8). Once these corrections have been obtained, physical observables like the Josephson current may be computed via the free energy $F = -\frac{1}{\beta}\ln(Z)$, with β the inverse temperature. Therefore, it is most convenient to work in an action-based description, which directly yields the partition function Z. Following Ref. 21, we first integrate over the fermions in the leads. Omitting the resulting irrelevant constant, the partition function reads

$$Z = \int \mathcal{D}(\bar{\Psi}_d, \Psi_d) e^{-S_{\mathrm{dot}}} \qquad (12)$$

with

$$\begin{aligned}
S_{\mathrm{dot}} = &\sum_{\vec{k},i,\omega_n} \bar{\Psi}_{d,n} \hat{H}_{T_i} \hat{G}^0_{\vec{k}i,\vec{k}i}(i\omega_n) \hat{H}_{T_i}^\dagger \Psi_{d,n} \\
&+ \sum_{\omega_n} \bar{\Psi}_{d,n} \begin{pmatrix} -i\omega_n + \epsilon_d & 0 \\ 0 & -i\omega_n - \epsilon_d \end{pmatrix} \Psi_{d,n} \\
&+ \int_0^\beta d\tau U \bar{d}_\uparrow(\tau) \bar{d}_\downarrow(\tau) d_\downarrow(\tau) d_\uparrow(\tau),
\end{aligned} \qquad (13)$$

where we have introduced the Grassmann Nambu spinors at Matsubara frequency $\omega_n = (2n+1)\pi/\beta$,

$$\Psi_{d,n} = \frac{1}{\sqrt{\beta}} \sum_{\omega_n} \begin{bmatrix} d_\uparrow(\tau) \\ \bar{d}_\downarrow(\tau) \end{bmatrix} e^{-i\omega_n \tau}$$

and

$$\bar{\Psi}_{d,n} = \frac{1}{\sqrt{\beta}} \sum_{\omega_n} [\bar{d}_\uparrow(\tau), \ d_\downarrow(\tau)] e^{i\omega_n \tau},$$

denoting the Grassmann fields associated with electrons in the dot by $\bar{d}_\sigma$ and d_σ.

The perturbation consists of the terms in Eq. (12) that are not contained in the action S_{eff} corresponding to the effective local Hamiltonian. A simple identification yields

$$\begin{aligned}
S_{\mathrm{eff}} = \int_0^\beta d\tau \bigg[&\sum_\sigma \bar{d}_\sigma(\tau) \left(\frac{\partial}{\partial \tau} + \epsilon_d \right) d_\sigma(\tau) - |\Gamma_\varphi| \bar{d}_\uparrow(\tau) \bar{d}_\downarrow(\tau) \\
&- |\Gamma_\varphi| d_\downarrow(\tau) d_\uparrow(\tau) + U \bar{d}_\uparrow(\tau) \bar{d}_\downarrow(\tau) d_\downarrow(\tau) d_\uparrow(\tau) \bigg],
\end{aligned} \qquad (14)$$

$$\begin{aligned}
S_{\mathrm{pert}} = \int_0^\beta d\tau \int_0^\beta d\tau' &\sum_{\vec{k},i} \bar{\Psi}_d(\tau) \hat{H}_{T_i} \hat{G}^0_{\vec{k}i,\vec{k}i}(\tau - \tau') \hat{H}_{T_i}^\dagger \Psi_d(\tau') \\
&+ \int_0^\beta d\tau [|\Gamma_\varphi| \bar{d}_\uparrow(\tau) \bar{d}_\downarrow(\tau) + |\Gamma_\varphi| d_\downarrow(\tau) d_\uparrow(\tau)].
\end{aligned} \qquad (15)$$

Note that S_{eff} contains the local-pairing term derived in Sec. II B. The proximity effect is thus treated nonperturbatively (just like the Coulomb interaction), which is the crucial ingredient of our analytic approach. The perturbation S_{pert} simply corresponds to the tunnel coupling between the dot and the electrodes other than the lowest-order proximity effect.

The actual corrections are calculated by expanding the partition function to the first order in S_{pert} according to

$$Z = \int \mathcal{D}(\bar{\Psi}, \Psi) e^{-S_{\mathrm{eff}} - S_{\mathrm{pert}}} \approx \int \mathcal{D}(\bar{\Psi}, \Psi) e^{-S_{\mathrm{eff}}} (1 - S_{\mathrm{pert}} + \cdots) \qquad (16)$$

which we then identify with

$$Z = \sum_\sigma e^{-\beta E_\sigma} + e^{-\beta E_+} + e^{-\beta E_-}, \tag{17}$$

where the renormalized superconducting atomic levels $E_\sigma = E_\sigma^0 + \delta E_\sigma$ and $E_\pm = E_\pm^0 + \delta E_\pm$ are obtained from

$$e^{-\beta E_\sigma} \approx e^{-\beta E_\sigma^0}(1 - \beta \delta E_\sigma), \tag{18}$$

$$e^{-\beta E_\pm} \approx e^{-\beta E_\pm^0}(1 - \beta \delta E_\pm). \tag{19}$$

Because the Coulomb interaction is taken into account, Wick's theorem cannot be used to calculate Z. Instead, expectation values are calculated using Lehmann representation. Explicit calculations may be found in the Appendix. In the zero-temperature limit $\beta \to \infty$, the energy corrections are

$$\delta E_\sigma = -t^2 \sum_{\vec{k}} \left\{ \frac{1}{E_{\vec{k}} + (E_+^0 - E_\sigma^0)} + \frac{1}{E_{\vec{k}} + (E_-^0 - E_\sigma^0)} \right.$$
$$+ \frac{2\Delta}{E_{\vec{k}}} uv \left| \cos\left(\frac{\varphi}{2}\right) \right| \left[\frac{1}{E_{\vec{k}} + (E_+^0 - E_\sigma^0)} \right.$$
$$\left. \left. - \frac{1}{E_{\vec{k}} + (E_-^0 - E_\sigma^0)} \right] \right\}, \tag{20}$$

$$\delta E_+ = -t^2 \sum_{\vec{k},\sigma} \left[\frac{1}{E_{\vec{k}} - (E_+^0 - E_\sigma^0)} \right.$$
$$\left. - \frac{2\Delta}{E_{\vec{k}}} uv \left| \cos\left(\frac{\varphi}{2}\right) \right| \frac{1}{E_{\vec{k}} - (E_+^0 - E_\sigma^0)} \right] - 2|\Gamma_\varphi| uv, \tag{21}$$

$$\delta E_- = -t^2 \sum_{\vec{k},\sigma} \left[\frac{1}{E_{\vec{k}} - (E_-^0 - E_\sigma^0)} \right.$$
$$\left. + \frac{2\Delta}{E_{\vec{k}}} uv \left| \cos\left(\frac{\varphi}{2}\right) \right| \frac{1}{E_{\vec{k}} - (E_-^0 - E_\sigma^0)} \right] + 2|\Gamma_\varphi| uv, \tag{22}$$

with the quasiparticle energy $E_{\vec{k}} = \sqrt{\epsilon_{\vec{k}}^2 + \Delta^2}$.

B. Self-consistent renormalization of the energy

Equations (20)–(22) yield the first corrections to the energy levels so that the bound-states energies a_0 and b_0 are simply shifted by $\delta a = \delta E_- - \delta E_\sigma$ and $\delta b = \delta E_+ - \delta E_\sigma$. Obviously, these expressions are logarithmically divergent when the bound-states energies a_0 and b_0 approach the gap edge[35] and are therefore only valid as long as, e.g., $a_0 \gg \Gamma \log[(D+\Delta)/(\Delta - a_0)]$. In the limit of large gap $\Delta \gg a_0$, these corrections to a_0 are thus of the order $\Gamma a_0/\Delta$ so that the small dimensionless parameter is indeed Γ/Δ. However, this peculiar logarithmic dependence of the ABS energy renormalization shows that doing a straightforward $1/\Delta$ expansion around the effective local Hamiltonian will be rapidly uncontrolled and will have a hard time reproducing the logarithmic singularities at Δ close to a_0. For this reason and also because the large-gap limit becomes trivial for a finite elec-
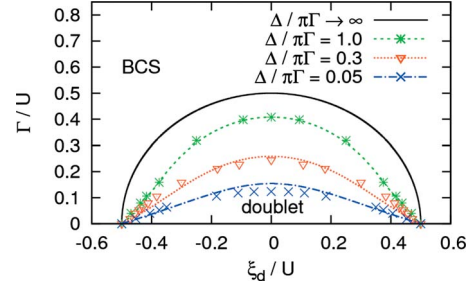

FIG. 2. (Color online) Phase diagram of a simple dot with Coulomb interaction U, tunnel coupling Γ to superconducting electrodes with gap Δ for $\varphi = 0$ and $\pi\Gamma = 0.2D$. The symbols indicate NRG data from Ref. 2 and the various lines our results.

tronic bandwidth, as discussed in Sec. II B, it was indeed more appropriate to single out in the total action all terms left over with respect to the local superconducting effective Hamiltonian, see Eq. (15), and do perturbation theory around these.

Because our lowest-order expansion obviously still breaks down when the gap becomes comparable to the bound-state energy, one would naturally seek to resum the leading logarithmic divergences in Eqs. (20)–(22). This can be achieved using a self-consistency condition inspired by Brillouin-Wigner perturbation theory,[47] which allows to extend greatly the regime of validity of the perturbative scheme. The resulting self-consistent equations that we obtain are

$$\delta a = -\frac{\Gamma}{\pi} \int_0^D d\epsilon \left\{ \frac{2}{E - a(\Delta)} - \frac{1}{E + b_0} - \frac{1}{E + a_0} \right.$$
$$\left. + \frac{\Delta}{E} uv \left| \cos\left(\frac{\varphi}{2}\right) \right| \left[\frac{2}{E - a(\Delta)} - \frac{1}{E + b_0} + \frac{1}{E + a_0} \right] \right\}$$
$$+ 2|\Gamma_\varphi| uv \tag{23}$$

and

$$\delta b = -\frac{\Gamma}{\pi} \int_0^D d\epsilon \left\{ \frac{2}{E - b(\Delta)} - \frac{1}{E + b_0} - \frac{1}{E + a_0} \right.$$
$$\left. + \frac{\Delta}{E} uv \left| \cos\left(\frac{\varphi}{2}\right) \right| \left[\frac{-2}{E - b(\Delta)} - \frac{1}{E + b_0} + \frac{1}{E + a_0} \right] \right\}$$
$$- 2|\Gamma_\varphi| uv \tag{24}$$

with $E = \sqrt{\epsilon^2 + \Delta^2}$, and a_0, b_0 have been defined in Eqs. (10) and (11), with $a(\Delta) = a_0 + \delta a$, $b(\Delta) = b_0 + \delta b$. Note that terms like $1/(E + a_0)$ have no self-consistency because there are no associated divergences. Equations (23) and (24) clearly now hold as long as the *renormalized* energies $a(\Delta)$ and $b(\Delta)$ are not too close to the gap edge, $\pm\Delta$, respectively.

IV. RESULTS

A. Phase diagram

We start by discussing the 0-π transition line, by comparison to the NRG data by Bauer *et al.*[2] Figure 2 shows the extension to smaller gaps Δ values of the phase diagram
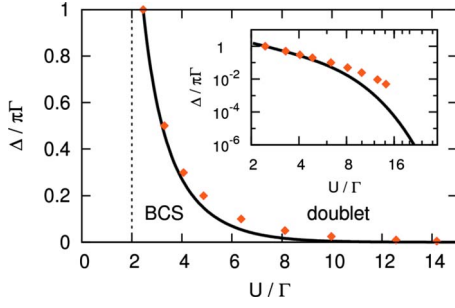
FIG. 3. (Color online) Transition line between a doublet state and the BCS-type state at particle-hole symmetry $\xi_d=0$ (solid curve) for $\varphi=0$ and $\pi\Gamma=0.2D$. The vertical dotted line corresponds to the transition asymptote in the effective local limit at $\Delta \to \infty$. The dots indicate NRG data from Ref. 2 and the solid line our result. The inset displays the same curves on a logarithmic scale.

obtained with unrenormalized local superconducting states for infinite gap (Fig. 1). Even though our perturbative approach is fairly simple, the results reproduce nicely the NRG data of Refs. 2 and 27. The analytically obtained phase diagram is indeed identical to the NRG data for $\Delta \gtrsim \Gamma$. For smaller Δ/Γ, the Kondo effect sets in but the transition lines remain quantitatively correct for ξ_d near $\pm U/2$ with increasing deviations from the NRG calculations close to the particle-hole symmetric point $\xi_d=0$ at large Coulomb interaction U. In this regime, the zero phase possesses a Kondo-singlet ground state. As the leads are superconductors, the formation of a Kondo resonance involves the breaking of Cooper pairs. Therefore, the transition is now due to the competition between T_K and the superconducting gap Δ, and should occur at $k_B T_K \propto \Delta$.

Figure 3 shows a plot of the transition line for $\xi_d=0$ as obtained with Eq. (23) (solid curve). The vertical dotted line depicts the asymptote in the effective local limit. The symbols again correspond to NRG data.[2] The Kondo temperature is given by $T_K=0.182U\sqrt{8\Gamma/\pi U}e^{-\pi U/8\Gamma}$ (see, for example, Ref. 2). The inset shows on a log-log scale that our approach captures an exponential decay of the transition line with the Coulomb interaction. Nonetheless, the suppression of the BCS-like phase appears quantitatively stronger than expected: a factor 4 instead of 8 is found in the exponential factor of T_K. The reason for this is that the vertex renormalizations have not been taken into account, as discussed in the context of U-NCA.[48] Far away from the particle-hole symmetric limit, our results for the Kondo temperature reproduce the lowest-order scaling theory for the infinite U Anderson model,[49] and are in relatively good agreement with NRG data for all Δ/Γ values.

B. Energy renormalizations at particle-hole symmetry ($\xi_d=0$)

While Fig. 2 only indicates the transition line between the spin 1/2 doublet and the lowest BCS spin singlet, it is also instructive to look at the actual renormalization of the energy levels while varying the gap Δ from large values to smaller ones beyond the critical point. Figure 4 indicates the renormalized energies of the two Andreev bound states (i.e., the difference between the spin 1/2 doublet and the two spin-
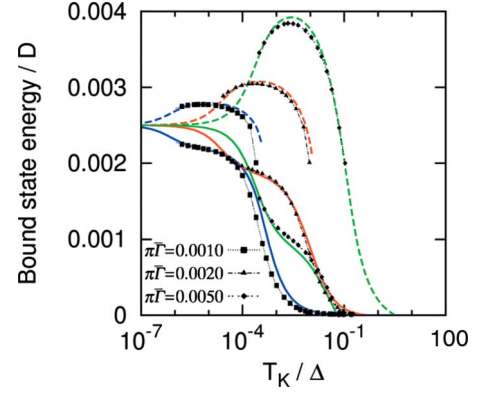

FIG. 4. (Color online) Renormalization of the Andreev bound-state energies as a function of T_K/Δ (the Kondo temperature is given in the text). The dashed curves correspond to the high-energy bound state $b(\Delta)$, the solid curves correspond to $a(\Delta)$. All curves have been calculated for $U=0.005D$ and $\xi_d=0$ with several hybridization values $\pi\Gamma/D=0.001,0.002,0.005$ (from left to right). Symbols are the NRG results obtained in Ref. 30.

singlets energies) for different hybridizations Γ. We note that our results are in quantitative agreement with the NRG calculations of Yoshioka and Ohashi.[30] Several regions need to be distinguished. If the gap Δ is much larger than the bandwidth D, all curves collapse at the value $U/2$ (left-hand side of Fig. 4) since there is no hybridization with both quasiparticles and Cooper pairs anymore, and one recovers the bare atomic levels. When the gap starts to decrease, the proximity effect simply splits the two Andreev bound states according to Eqs. (10) and (11). When the gap becomes of the same order as the typical energy scales of the dot a_0 and b_0, the superconducting atomic levels start to mix with the electrodes so that the energies renormalize in a nontrivial way. One can see that the transition involving the highest BCS states ends up touching the gap edge for $\Delta \approx U/2$ so that half of the ABS are absorbed into the continuum above Δ, as can be seen in Fig. 5. The lowest BCS state follows however a downward renormalization until the Fermi level is crossed and the ground state becomes the zero state. The difference in behavior between the lowest and highest bound states (the former being never allowed to leave the superconducting
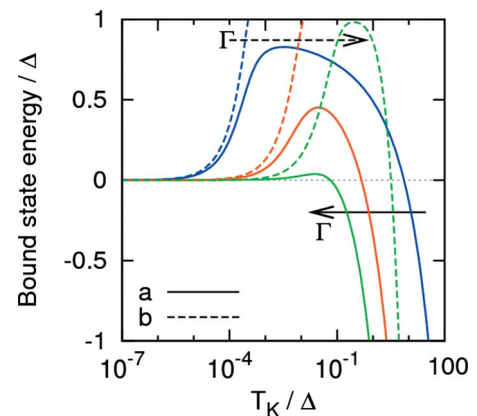

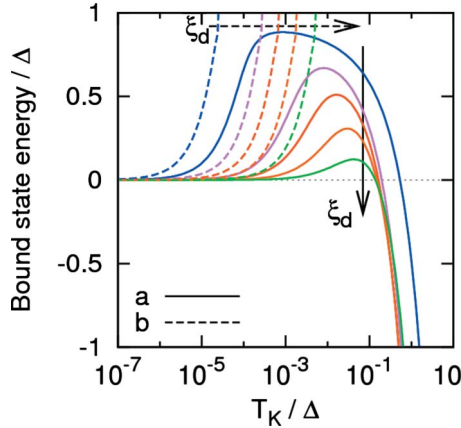FIG. 5. (Color online) Same data as in Fig. 4 but normalized by the gap.

FIG. 6. (Color online) Renormalization of the Andreev bound-state energies outside particle-hole symmetry. The dotted curves correspond to the high-energy bound state $b(\Delta)$, the solid curves correspond to $a(\Delta)$. All curves have been calculated for $U=0.5D$ and $\pi\Gamma=0.05D$ with several level shifts ξ_d/U $=0.3,0.375,0.4,0.425,0.45$. Quantitatively similar results were obtained by the NRG in Ref. 30.

gap) can be tracked into Eqs. (23) and (24), where level repulsion effects from the gap edge occur for the low energy level $|-\rangle$ but are canceled for the high energy level $|+\rangle$, which is hence allowed to penetrate into the continuum. These considerations unveil how the ABS may be adiabatically connected to the atomic (or molecular) levels in a complicated fashion.

Again, our simple analytic approach reproduces the NRG results[30] over a vast regime of parameters. Yet, some deviations are observed in the Kondo regime: we find (for the highest hybridization $\pi\Gamma=0.005D$) that the high-energy BCS-like state is not absorbed anymore into the continuum of states—an artifact of the limits of our perturbative approach. Notice also that the energy corrections are too important if the gap becomes very small, an effect actually due to our underestimation of the Kondo temperature at particle symmetry, as discussed previously. Finally Fig. 5 shows that, in the limit of vanishing gap, our approach is only valid as long as $a(\Delta) \gtrsim -\Delta$ (as has been mentioned in Sec. III B) because the lowest bound state artificially escapes from the gap. The expected saturation of $a(\Delta)$ near $-\Delta$ can be restored by adding a further self-consistency for terms such as $1/(E +a_0)$ in Eq. (23) (not shown here).

C. Energy renormalizations outside particle-hole symmetry ($\xi_d \neq 0$)

From an experimental point of view, the position of the energy level of the quantum dot is the most controllable parameter of the system (by a simple gate voltage). Therefore, it is important to analyze the evolution of the Andreev bound states for different values of ξ_d.

Figure 6 illustrates how the energies of the bound states scale with Δ for $\xi_d \neq 0$ and can be favorably compared to the NRG data by Yoshioka and Ohashi.[30] The more particle-hole symmetry is broken, the more the low-energy bound state moves away from the gap edge, ensuring even better conver-
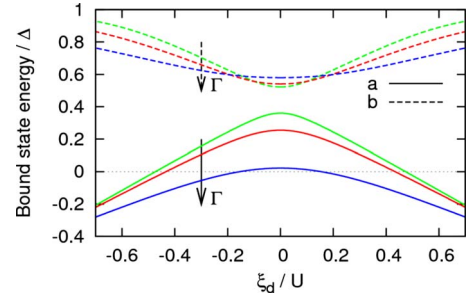

FIG. 7. (Color online) Evolution of the Andreev bound-state energies as a function of the dot's energy level for $U=0.005D$ and $\Delta=U$. The hybridization takes several values $\pi\Gamma/D$ $=0.001,0.002,0.005$.

gence of our expansion for a given value of Γ. This can be understood given that this bound state corresponds to the transition between $|-\rangle$ and the spin 1/2 doublet: outside particle-hole symmetry, the dot either seeks to be as empty as possible (for $\xi_d>0$) or as occupied as possible (for $\xi_d<0$). Thus, a BCS-like wave function will be favored. As a consequence, the Kondo effect (that necessitates a singly occupied dot) is less favored. This corresponds to a regime where our approximation scheme works at best.

Further understanding can be gained by looking at the energies of the Andreev bound states as a function of ξ_d on Fig. 7. We recover the fact that the high-energy bound states increases in energy by breaking particle-hole symmetry whereas the low-energy bound state has a decreasing energy. In addition, Fig. 7 shows that the dispersion of both ABS weakens for increasing hybridization. Indeed, the more the dot is hybridized with the leads, the less the Andreev bound-state energy is sensitive to the bare values of the dot parameters.

D. Superconducting correlations on the dot

In order to further analyze the evolution of the states in the dot as a function of the parameters in the model in Eq. (1), we investigate now the superconducting correlations $\langle d_\uparrow^\dagger d_\downarrow^\dagger \rangle$ on the dot. For the effective local Hamiltonian, these correlations are zero in the spin-doublet phase. In the BCS-like phase, the correlations are maximal if the two states $|0\rangle$ and $|\uparrow\downarrow\rangle$ are equivalent, i.e., at particle-hole symmetry. If the dot level is far from $\xi_d=0$, the wave function will be predominantly $|0\rangle$ (if ξ_d is positive) or $|\uparrow\downarrow\rangle$ (if ξ_d is negative). This obviously kills the superconducting correlations.

As the gap decreases from infinity, the (formerly) singly occupied state will start having a BCS-like admixture and therefore a nonzero superconducting correlation. In contrast, the mixing will result in a decreased correlation in the BCS-like phase. Nevertheless, if the gap tends to zero, one would expect the correlations to vanish as well. This is indeed what Fig. 8 shows. For large gaps, the dot is in the spin 1/2 phase; the correlations are small but increase as the states mix. The transition to the BCS-like phase results in a discontinuous jump in the correlations, before they finally vanish for very small gaps. It can thus be concluded that the correlations should be normalized by the gap if one is interested in mea-
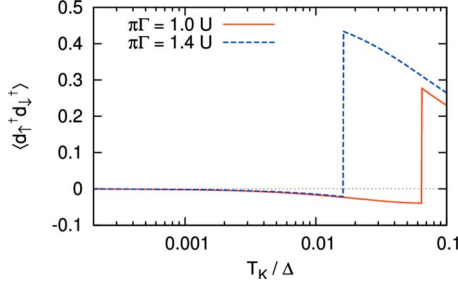
FIG. 8. (Color online) Superconducting correlations as a function of the gap Δ (for $U=D/200$ and $\xi_d=0$).

FIG. 10. (Color online) Superconducting correlations outside particle-hole symmetry (for $\pi\Gamma=0.2D$, $U=6\Gamma$, and $\Delta=0.1D$).

suring only the mixing effect. Finally, the two different curves show how hybridization stabilizes the BCS-like state with respect to the spin doublet via the $0-\pi$ transition.

As the Coulomb interaction tries to prevent the formation of a Cooper-pair wave function, the transition between the BCS-like phase and the spin doublet can also be achieved if the Coulomb interaction is tuned, as shown in Fig. 9. The effect of the mixing is clearly visible by an increase in the correlation $\langle d_\uparrow^\dagger d_\downarrow^\dagger \rangle$ (now normalized by the gap) while U is lowered. We also find that the correlations relative to the gap decrease for higher gaps, which is a simple saturation effect (the highest possible correlations are $\langle d_\uparrow^\dagger d_\downarrow^\dagger \rangle=0.5$). Furthermore, our results are quantitatively precise if the gap if larger than the hybridization Γ for all values of U while relatively small deviations appear for $\Delta<\pi\Gamma$, as shown by the comparison to the NRG data from Ref. 2 and to second-order perturbation theory in U (valid in the singlet phase only, providing accurate results for $U\lesssim 2\pi\Gamma$ roughly).[24,50]

Finally, we analyze how the correlations evolve outside particle-hole symmetry. As mentioned above, one expects the correlations to decrease because the dot evolve from a super-conducting atomic limit toward a usual atomic limit (i.e., from the states $|\pm\rangle$ toward the states $|0\rangle$ and $|\uparrow\downarrow\rangle$). On the other hand, there will be a transition from the spin doublet to the singlet phase and therefore a mixing effect. Figure 10 shows the competition between the mixing effect (that increases the correlations outside particle-hole symmetry) and the evolution toward the normal atomic limit (that lowers the correlations) if ξ_d is increased. The effect of the Coulomb interaction is once more found to favor the single occupancy.
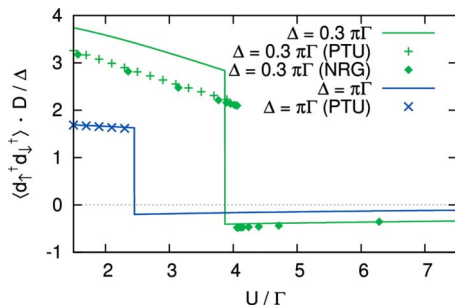
E. Josephson current

We now turn to the Josephson current through the quantum dot. The latter is given by $J=2e\frac{dF}{d\varphi}$ (where F is the free energy). At zero temperature, the free energy is the same than the level energies so that the Josephson current can readily be obtained once the renormalized energy levels have been calculated.

Nevertheless, our analytical approach only describes the effective local limit atomic states and we can therefore only determine the current through the Andreev bound states. Yet, it is known that the Josephson current also contains a contribution of the continuum of states.[3] The latter can be of the same order and opposite sign as the bound-state contribution. Furthermore, Bauer *et al.*[2] showed that the spectral weight of the bound states may vary importantly as a function of the different parameters (like the Coulomb interaction U), especially in the spin-doublet phase. As we exclusively investigate the effective local limit states, we do not keep track of this effect as well. Therefore, the Josephson currents obtained in our approach will only provide a rather rough and qualitative idea of the actual total Josephson current.

Figure 11 shows the Josephson current calculated as the phase derivative of the ground-state energy E_x, $J=\frac{dE_x}{d\varphi}$, for different values of ξ_d. One notices two regimes: If the phase is close to $\varphi=0$, the system will be in the BCS-like state. As there is no magnetic moment in this phase, the ground state corresponds to a zero junction (i.e., phase difference $\varphi=0$). If φ increases, the energy of the BCS-type state increases (as can be understood in the effective local limit, where $E_-=U/2-\sqrt{\xi_d^2+\Gamma_\varphi^2}$). When the BCS-like state crosses with the spin doublet, the ground state changes and the dot becomes singly occupied. This magnetic moment leads to a discon-

FIG. 9. (Color online) Superconducting correlations as a function of the Coulomb interaction U, for $\Delta/(\pi\Gamma)=0.3,1.0$ and at particle-hole symmetry $\xi_d=0$. Solid lines are the results of our self-consistent equations, diamonds correspond to NRG data from Ref. 2, and crosses are perturbation theory in U at second order.
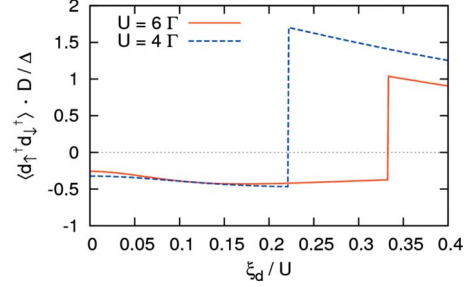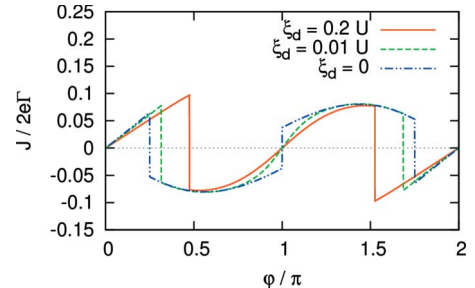

FIG. 11. (Color online) Josephson current through the bound states for $U=3\Gamma$ and $\Delta=0.1D$.

tinuous jump in the Josephson current and the formation of a π junction. Again, we notice that the spin doublet is stabilized in the particle-hole symmetric case.

V. CONCLUSION

In this section we summarize our main results. First, it has been shown how the Hamiltonian of a quantum dot coupled to superconducting leads can be mapped onto an effective local model if the superconducting gap Δ is much bigger than the characteristic energy scales of the dot. This limit can be quite generally regarded as a low-frequency expansion of the Green's function of the dot rather than the limit $\Delta \to \infty$ used in the literature. This enabled us to extend the effective local Hamiltonian to leads with a finite electronic bandwidth.

We have then set up a perturbation theory around this local effective Hamiltonian and established self-consistent equations for the energy renormalizations of the Andreev bound states. We have derived those equations based on the fact that the latter correspond to transitions between different states of the local effective Hamiltonian.

In the last section, we used our formalism to calculate physical quantities such as the Andreev bound-state energies or superconducting correlations, and understood how these evolve as a function of gate voltage, hybridization, Coulomb interaction, and superconducting gap amplitude. It has been shown that our simple approach agrees well with NRG data in a vast range of parameters with the main limitation that the Kondo temperature is not quantitatively described near particle-hole symmetry. However, most experimentally interesting regimes should be described correctly by the simple equations we have derived.

The simplicity and portability constitute the main advantages of our approach if one is interested in the Andreev bound states only, compared to extended numerical simulations. As the perturbative description is analytical and based on atomiclike levels, it should, in principle, be able to describe more complex systems like multiple quantum dots or molecules with several orbitals coupled to superconducting environments and be readily applicable to describe future spectroscopic measurements. Extensions of our formalism to the computation of the tunneling current at realistic gap values in three-terminal geometries[6] relevant for STM experiments should certainly deserve further scrutiny.

ACKNOWLEDGMENTS

APPENDIX: DERIVATION OF THE ENERGY CORRECTIONS

The partition function is derived starting from the action's perturbation expansion in Sec. III. The actual calculations are performed in the operator formalism. It is very useful to note that the product of two fermionic (or bosonic) Green's functions $G_a(\tau)$ and $G_b(\tau)$ obeys $\int_0^\beta d\tau \int_0^\beta d\tau' G_a(\tau-\tau')G_b(\tau-\tau')$

$= \beta \int_0^\beta d\tau G_a(\tau)G_b(\tau)$ (as can be shown using Fourier transformation). The partition function's perturbation expansion is

$$
\begin{aligned}
Z = Z_0 - Z_0 t^2 \beta \sum_{\vec{k},i} \int_0^\beta d\tau & [G^0_{\vec{k}i\vec{k}i;11}(\tau)\langle T_\tau d^\dagger_\uparrow(\tau)d_\uparrow(0)\rangle_0 \\
& - G^0_{\vec{k}i\vec{k}i;12}(\tau)\langle T_\tau d^\dagger_\uparrow(\tau)d^\dagger_\downarrow(0)\rangle_0 - G^0_{\vec{k}i\vec{k}i;21}(\tau)\langle T_\tau d_\downarrow(\tau)d_\uparrow(0)\rangle_0 \\
& + G^0_{\vec{k}i\vec{k}i;22}(\tau)\langle T_\tau d_\downarrow(\tau)d^\dagger_\downarrow(0)\rangle_0] - 2\beta|\Gamma_\varphi|[\langle T_\tau d^\dagger_\uparrow(0)d^\dagger_\uparrow(0)\rangle_0 \\
& + \langle T_\tau d_\downarrow(\tau)d_\uparrow(0)\rangle_0].
\end{aligned}
\tag{A1}
$$

In the above equation, $G^0_{\vec{k}i\vec{k}i;ij}$ is the Fourier-transformed Nambu matrix element $\hat{G}^0_{\vec{k}i,\vec{k}i}(i\omega_n)|_{i,j}$ and the subscript zero indicates that the expectation values are statistical averages calculated in the effective local limit. The leads' Green's functions are

$$
\sum_{\vec{k}} G^0_{\vec{k}i\vec{k}i;11}(\tau) = \sum_{\vec{k}} - \frac{\text{sgn}(\tau)}{2}(e^{-|\tau|E^-_{\vec{k}}} + e^{-(\beta-|\tau|)E_{\vec{k}}}),
$$

$$
G^0_{\vec{k}i\vec{k}i;12}(\tau)e^{-i\varphi_i} = \frac{\Delta}{2E_{\vec{k}}}(e^{-|\tau|E_{\vec{k}}} - 2\cosh(|\tau|E)n_F(E_{\vec{k}}))
$$

$$
\xrightarrow{T\to 0\text{K}} \frac{\Delta}{2E_{\vec{k}}}(e^{-|\tau|E_{\vec{k}}} - e^{-(\beta-|\tau|)E_{\vec{k}}})
$$

with $E_{\vec{k}} = \sqrt{\epsilon^2_{\vec{k}} + \Delta^2}$. Furthermore, $G^0_{\vec{k}i\vec{k}i;21}(\tau) = G^0_{\vec{k}i\vec{k}i;12}(\tau)^*$ and $\Sigma_{\vec{k}} G^0_{\vec{k}i\vec{k}i;22}(\tau) = \Sigma_{\vec{k}} G^0_{\vec{k}i\vec{k}i;11}(\tau)$.

As one cannot apply Wick's theorem because of the Coulomb interaction, the dot's Green's functions are calculated using Lehmann representation, which yields (for $\tau > 0$)

$$
\begin{aligned}
\langle T_\tau d^\dagger_\uparrow(\tau)d_\uparrow(0)\rangle_0 = \frac{1}{Z_0}\{&u^2[e^{-E^0_-\tau}e^{-E^0_\uparrow(\beta-\tau)} + e^{-E^0_\downarrow\tau}e^{-E^0_+(\beta-\tau)}] \\
& + v^2[e^{-E^0_+\tau}e^{-E^0_\uparrow(\beta-\tau)} + e^{-E^0_\downarrow\tau}e^{-E^0_-(\beta-\tau)}]\},
\end{aligned}
\tag{A2}
$$

$$
\begin{aligned}
\langle T_\tau d^\dagger_\uparrow(\tau)d^\dagger_\downarrow(0)\rangle_0 = \frac{1}{Z_0}uv(&e^{-E^0_\downarrow\tau}e^{-E^0_-(\beta-\tau)} - e^{-E^0_-\tau}e^{-E^0_\uparrow(\beta-\tau)} \\
& - e^{-E^0_\downarrow\tau}e^{-E^0_+(\beta-\tau)} + e^{-E^0_+\tau}e^{-E^0_\uparrow(\beta-\tau)}),
\end{aligned}
\tag{A3}
$$

$$
\begin{aligned}
\langle T_\tau d_\downarrow(\tau)d_\uparrow(0)\rangle_0 = \frac{1}{Z_0}uv(&e^{-E^0_\downarrow\tau}e^{-E^0_-(\beta-\tau)} - e^{-E^0_-\tau}e^{-E^0_\uparrow(\beta-\tau)} \\
& - e^{-E^0_\downarrow\tau}e^{-E^0_+(\beta-\tau)} + e^{-E^0_+\tau}e^{-E^0_\uparrow(\beta-\tau)}),
\end{aligned}
\tag{A4}
$$

$$
\begin{aligned}
\langle T_\tau d_\downarrow(\tau)d^\dagger_\downarrow(0)\rangle_0 = \frac{1}{Z_0}\{&u^2[e^{-E^0_-\tau}e^{-E^0_\uparrow(\beta-\tau)} + e^{-E^0_\downarrow\tau}e^{-E^0_-(\beta-\tau)}] \\
& + v^2[e^{-E^0_-\tau}e^{-E^0_\uparrow(\beta-\tau)} + e^{-E^0_\downarrow\tau}e^{-E^0_+(\beta-\tau)}]\}.
\end{aligned}
\tag{A5}
$$

Using $u^2 + v^2 = 1$, the partition function becomes

$$Z = Z_0 + \beta t^2 \sum_{\vec{k},\sigma} \times \left(\frac{1}{E - (E_+^0 - E_\sigma^0)}(e^{-\beta E_+^0} - e^{-\beta(E+E_\sigma^0)}) + \frac{1}{E - (E_-^0 - E_\sigma^0)}[e^{-\beta E_-^0} - e^{-\beta(E+E_\sigma^0)}] + \frac{1}{E + (E_+^0 - E_\sigma^0)}[e^{-\beta E_\sigma^0} - e^{-\beta(E+E_+^0)}] \right.$$

$$+ \frac{1}{E + (E_-^0 - E_\sigma^0)}[e^{-\beta E_\sigma^0} - e^{-\beta(E+E_-^0)}] + \frac{2\Delta}{E} uv \left| \cos\left(\frac{\varphi}{2}\right) \right| \left\{ \frac{1}{E + (E_+^0 - E_\sigma^0)}[e^{-\beta E_\sigma^0} - e^{-\beta(E+E_+^0)}] - \frac{1}{E + (E_-^0 - E_\sigma^0)}[e^{-\beta E_\sigma^0} - e^{-\beta(E+E_-^0)}] \right.$$

$$\left. \left. - \frac{1}{E - (E_+^0 - E_\sigma^0)}[e^{-\beta E_+^0} - e^{-\beta(E+E_\sigma^0)}] + \frac{1}{E - (E_-^0 - E_\sigma^0)}[e^{-\beta E_-^0} - e^{-\beta(E+E_\sigma^0)}] \right\} \right) + 2\beta|\Gamma_\varphi| uv(e^{-\beta E_+^0} - e^{-\beta E_-^0}). \tag{A6}$$

As $E_{\vec{k}} = \sqrt{\epsilon_{\vec{k}}^2 + \Delta^2} > 0$, terms with an $e^{-\beta E_{\vec{k}}}$ are exponentially suppressed for $T \to 0$ K and can be omitted.

[1] C. W. J. Beenakker and H. van Houten, in *Single-Electron Tunneling and Mesoscopic Devices*, edited by H. Koch and H. Lübbig (Springer, Berlin, 1992); arXiv:cond-mat/0111505.

[2] J. Bauer, A. Oguri, and A. C. Hewson, J. Phys.: Condens. Matter **19**, 486211 (2007).

[3] C. Benjamin, T. Jonckheere, A. Zazunov, and T. Martin, Eur. Phys. J. B **57**, 279 (2007).

[4] J. M. Rowell, Phys. Rev. Lett. **30**, 167 (1973).

[5] A. Zazunov, V. S. Shumeiko, E. N. Bratus, J. Lantz, and G. Wendin, Phys. Rev. Lett. **90**, 087003 (2003).

[6] M. Governale, M. G. Pala, and J. Konig, Phys. Rev. B **77**, 134513 (2008).

[7] J. Sköldberg, T. Löfwander, V. S. Shumeiko, and M. Fogelström, Phys. Rev. Lett. **101**, 087002 (2008).

[8] P. Recher, Y. Nazarov, and L. Kouwenhoven, arXiv:0902.4468 (unpublished).

[9] I. A. Sadovskyy, G. B. Lesovik, and G. Blatter, Phys. Rev. B **75**, 195334 (2007).

[10] C. Buizert, A. Oiwa, K. Shibata, K. Hirakawa, and S. Tarucha, Phys. Rev. Lett. **99**, 136806 (2007).

[11] M. R. Buitelaar, T. Nussbaumer, and C. Schönenberger, Phys. Rev. Lett. **89**, 256801 (2002).

[12] H. I. Jørgensen, K. Grove-Rasmussen, T. Novotný, K. Flensberg, and P. E. Lindelof, Phys. Rev. Lett. **96**, 207003 (2006).

[13] P. Jarillo-Herrero, J. A. van Dam, and L. P. Kouwenhoven, Nature (London) **439**, 953 (2006).

[14] M. R. Buitelaar, W. Belzig, T. Nussbaumer, B. Babic, C. Bruder, and C. Schönenberger, Phys. Rev. Lett. **91**, 057005 (2003).

[15] A. Y. Kasumov, R. Deblock, M. Kociak, B. Reulet, H. Bouchiat, I. I. Khodos, Y. B. Gorbatov, V. T. Volkov, C. Journet, and M. Burghard, Science **284**, 1508 (1999).

[16] L. I. Glazman and K. A. Matveev, JETP Lett. **49**, 659 (1989).

[17] J. J. A. Baselmans, A. F. Morpurgo, B. J. van Wees, and T. M. Klapwijk, Nature (London) **397**, 43 (1999).

[18] J. A. van Dam, Y. V. Nazarov, E. P. A. M. Bakkers, S. De Franceschi, and L. P. Kouwenhoven, Nature (London) **442**, 667 (2006).

[19] J. P. Cleuziou, W. Wernsdorfer, V. Bouchiat, T. Ondarçuhu, and M. Monthioux, Nat. Nanotechnol. **1**, 53 (2006).

[20] A. Eichler, R. Deblock, M. Weiss, C. Karrasch, V. Meden, C. Schönenberger, and H. Bouchiat, Phys. Rev. B **79**, 161407(R) (2009).

[21] A. V. Rozhkov and D. P. Arovas, Phys. Rev. Lett. **82**, 2788 (1999).

[22] Y. Avishai, A. Golub, and A. D. Zaikin, Phys. Rev. B **63**, 134515 (2001).

[23] L. Dell'Anna, A. Zazunov, and R. Egger, Phys. Rev. B **77**, 104525 (2008).

[24] E. Vecino, A. Martin-Rodero, and A. Levy Yeyati, Phys. Rev. B **68**, 035105 (2003).

[25] A. A. Clerk and V. Ambegaokar, Phys. Rev. B **61**, 9109 (2000).

[26] S. Ishizaka, J. Sone, and T. Ando, Phys. Rev. B **52**, 8358 (1995).

[27] C. Karrasch, A. Oguri, and V. Meden, Phys. Rev. B **77**, 024517 (2008).

[28] A. Oguri, Y. Tanaka, and A. C. Hewson, J. Phys. Soc. Jpn. **73**, 2494 (2004).

[29] M.-S. Choi, M. Lee, K. Kang, and W. Belzig, Phys. Rev. B **70**, 020502(R) (2004).

[30] T. Yoshioka and Y. Ohashi, J. Phys. Soc. Jpn. **69**, 1812 (2000).

[31] T. Hecht, A. Weichselbaum, J. von Delft, and R. Bulla, J. Phys.: Condens. Matter **20**, 275213 (2008).

[32] F. Siano and R. Egger, Phys. Rev. Lett. **93**, 047002 (2004).

[33] K. Kusakabe, Y. Tanaka, and Y. Tanuma, Physica E **18**, 50 (2003).

[34] M. G. Pala, M. Governale, and J. Konig, New J. Phys. **9**, 278 (2007).

[35] R. Bauernschmitt, J. Siewert, Y. V. Nazarov, and A. A. Odintsov, Phys. Rev. B **49**, 4076 (1994).

[36] I. Affleck, J.-S. Caux, and A. M. Zagoskin, Phys. Rev. B **62**, 1433 (2000).

[37] A. V. Rozhkov and D. P. Arovas, Phys. Rev. B **62**, 6687 (2000).

[38] Y. Tanaka, A. Oguri, and A. C. Hewson, New J. Phys. **9**, 115 (2007).

[39] A. Zazunov, D. Feinberg, and T. Martin, Phys. Rev. Lett. **97**, 196801 (2006).

[40] A. Zazunov, A. Schulz, and R. Egger, Phys. Rev. Lett. **102**, 047002 (2009).

[41] D. Futterer, M. Governale, M. G. Pala, and J. Konig, Phys. Rev. B **79**, 054505 (2009).

[42] Y. Tanaka, N. Kawakami, and A. Oguri, Phys. Rev. B **78**, 035444 (2008).

[43] M.-S. Choi, C. Bruder, and D. Loss, Phys. Rev. B **62**, 13569 (2000).

[44] M. Lee, T. Jonckheere, and T. Martin, Phys. Rev. Lett. **101**, 146804 (2008).

[45] F. S. Bergeret, A. Levy Yeyati, and A. Martin-Rodero, Phys. Rev. B **74**, 132505 (2006).

[46] H. I. Jørgensen, T. Novotný, K. Grove-Rasmussen, K. Flensberg, and P. E. Lindelof, Nano Lett. **7**, 2441 (2007).

[47] T. V. Ramakrishnan and K. Sur, Phys. Rev. B **26**, 1798 (1982).

[48] K. Haule, S. Kirchner, J. Kroha, and P. Wölfle, Phys. Rev. B **64**, 155111 (2001).

[49] F. D. M. Haldane, Phys. Rev. Lett. **40**, 416 (1978).

[50] T. Meng, Diploma thesis, Universität Karlsruhe (2009).